1.0

1.1

1.25

4.5
2.8
3.2
3.6
4.0

2.5

2.2

2.0
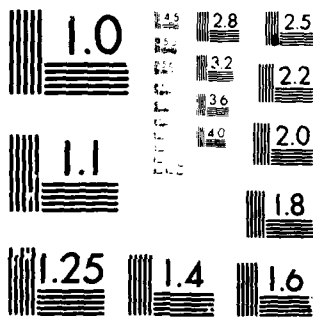
1.8

1.4

1.6

MICROCOPY RESOLUTION TEST CHART
NATIONAL BUREAU OF STANDARDS-1963-A

LEVEL

⑤

OFFICE OF NAVAL RESEARCH

Contract N00014-78-C-0591

Task No. NR 356-691

TECHNICAL REPORT NO. 1

The Feasibility of

Electrical Monitoring of Resin Cure with

the Charge-Flow Transistor

by

Stephen D. Senturia, Norman F. Sheppard,

Soon Y. Poh, and Howard R. Appelman

Prepared for Publication

in

Polymer Engineering and Science

MASSACHUSETTS INSTITUTE OF TECHNOLOGY

Department of Electrical Engineering and Computer Science

and Center for Materials Science and Engineering

Cambridge, Massachusetts

December 1, 1979

80 3 10 145

REPORT DOCUMENTATION PAGE		READ INSTRUCTIONS BEFORE COMPLETING FORM
1. REPORT NUMBER	2. GOVT ACCESSION NO.	3. RECIPIENT'S CATALOG NUMBER
4. TITLE (and Subtitle) The Feasibility of Electrical Monitoring of ⬛ Resin Cure with the Charge-Flow Transistor		5. TYPE OF REPORT & PERIOD COVERED Technical Report 4/78-9/79
		6. PERFORMING ORG. REPORT NUMBER Technical Report No. 1
7. AUTHOR(s) S.D. Senturia, N.F. Sheppard, S.Y. Poh, and H.R. Appelman		8. CONTRACT OR GRANT NUMBER(s) N00014-78-C-0591
9. PERFORMING ORGANIZATION NAME AND ADDRESS Massachusetts Institute of Technology Department of Electrical Engineering and Computer Science, Cambridge, Mass. 02139		10. PROGRAM ELEMENT, PROJECT, TASK AREA & WORK UNIT NUMBERS NR 356-691
11. CONTROLLING OFFICE NAME AND ADDRESS Department of the Navy Office of Naval Research 800 N. Quincy Street, Arlington, VA 22217 Code 472		12. REPORT DATE December1, 1979
		13. NUMBER OF PAGES 31
14. MONITORING AGENCY NAME & ADDRESS(if different from Controlling Office)		15. SECURITY CLASS. (of this report) UNCLASSIFIED
		15a. DECLASSIFICATION/DOWNGRADING SCHEDULE

16. DISTRIBUTION STATEMENT (of this Report)

This document has been approved for public release and sale; its distribution is unlimited.

17. DISTRIBUTION STATEMENT (of the abstract entered in Block 20, if different from Report)

18. SUPPLEMENTARY NOTES

19. KEY WORDS (Continue on reverse side if necessary and identify by block number)

Epoxy resin cure, charge-flow transistor, cure monitoring instrumentation

20. ABSTRACT (Continue on reverse side if necessary and identify by block number)

A new technique for the electrical monitoring of polymerization reactions such as resin cure is described. The technique is based on the charge-flow transistor, which resembles a conventional MOSFET, but with a portion of the metal gate replaced by the resin under study. Electrical signals obtained from several resins undergoing cure are presented, along with an electrical circuit model that can account for the principal features of these signals. The dramatic change in signal shape during cure can be related to corresponding changes in both the real and imaginary parts of the dielectric constant.

DD FORM 1473 EDITION OF 1 NOV 65 IS OBSOLETE
1 JAN 73
S/N 0102-LF-014-6601

THE FEASIBILITY OF ELECTRICAL MONITORING

OF RESIN CURE WITH THE CHARGE-FLOW TRANSISTOR

Stephen D. Senturia, Norman F. Sheppard,
Soon Y. Poh, and Howard R. Appelman

Department of Electrical Engineering and Computer Science,
Center for Materials Science and Engineering
Massachusetts Institute of Technology
Cambridge, Massachusetts   02139

ABSTRACT

A new technique for the electrical monitoring of polymerization reactions such as resin cure is described. The technique is based on the charge-flow transistor, which resembles a conventional MOSFET, but with a portion of the metal gate replaced by the resin under study. Electrical signals obtained from several resins undergoing cure are presented, along with an electrical circuit model that can account for the principal features of these signals. The dramatic change in signal shape during cure can be related to corresponding changes in both the real and imaginary parts of the dielectric constant.

i

TABLE OF CONTENTS

LIST OF FIGURES

I.   INTRODUCTION

The possibility of using the charge-flow transistor [1] to monitor polymerization reactions, such as the cure of epoxy resins, has been recognized for several years [2]. Initial experiments by Appelman [3] demonstrated that at least phenomenologically, it was possible to correlate the charge-flow transistor's signals during cure with such major features as time to gelation. The present program is directed toward a more careful examination of this subject, first, to document the observed phenomena, second, to develop models that can account for observed behavior, and third, to make explicit and quantitative correlations between the observed behavior during cure and the changing properties of the resin as evidenced by dielectric constant and loss tangent behavior. This report presents the first results of that effort.

The charge-flow transistor (CFT) is similiar to a conventional metal-oxide-semiconductor field-effect-transistor (FET), except that a portion of the gate metal is removed and is replaced by the sample of resin under study (see Fig. 1a). In effect, the resin serves as the transistor's gate electrode over a portion of the electrically sensitive channel region. The resin also coats the rest of the device, but it's electrical properties have a significant influence on device operation only in the gate-gap region, where the thin oxide permits charges in the vicinity of the resin-oxide interface to influence the conductivity of the channel through the well-known field effect. Typical device dimensions are as follows: The thin oxide is 1100 Å thick, the channel length between source and drain is 2 mils, and the gap width between two metallic

FIGURE 1

EPOXY

Gate-gap region

Metal

Gate electrode

Oxide

Source p⁺

Drain p⁺

Channel region

SUBSTRATE n-Si

(a)

Ammeter

CFT

S

G

D

V_g

V_d

Chart recorder
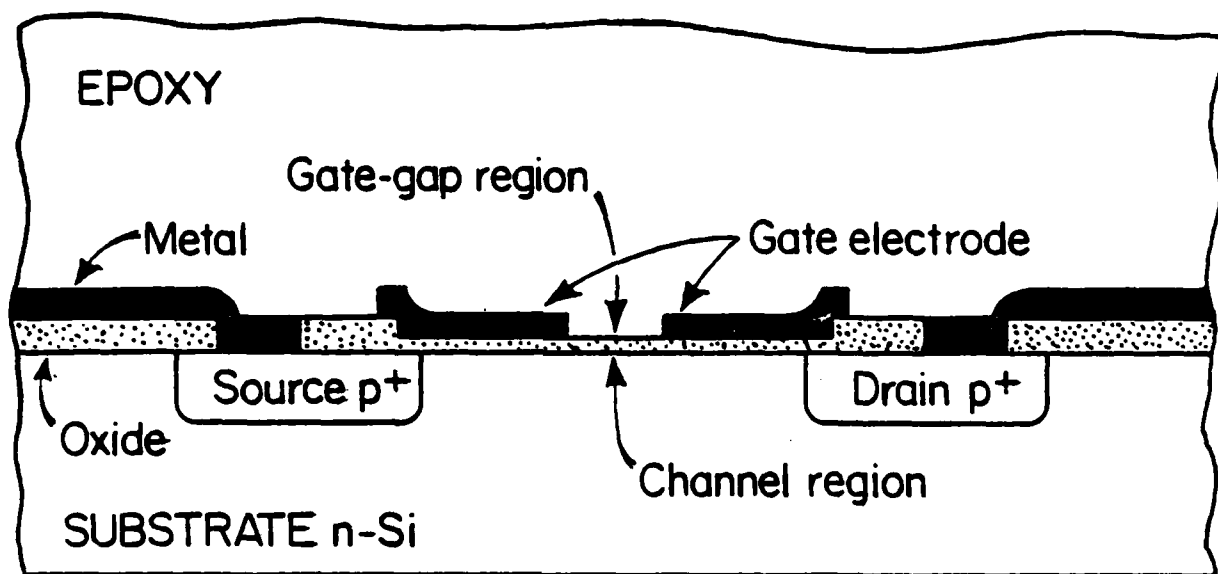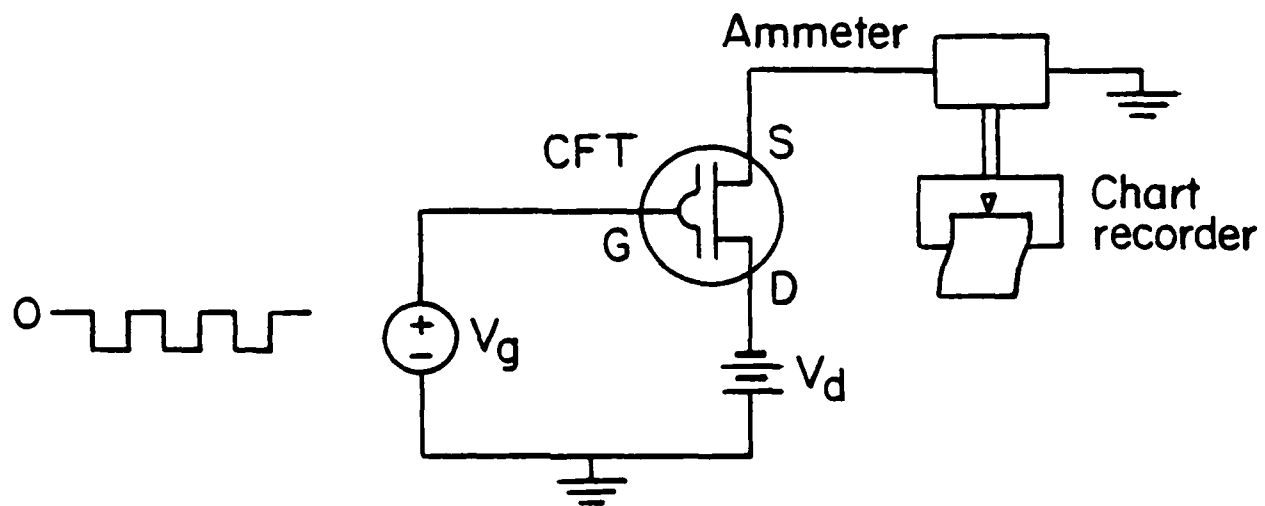
(b)

portions of the gate electrode varies from 0.25 mils to 1.50 mils. The channel width is 10 mils. The silicon substrate is n-type, and the source and drain regions are strongly p-type, leading to an enhancement mode p-channel device structure.

Typical use of the CFT is illustrated in Fig. 1b. The voltage applied to the gate electrode is switched alternately between ground and a voltage that is sufficiently negative to exceed the MOS threshold voltage of the device (our devices are p-channel, and hence require negative gate voltages). A small dc bias is applied to the drain, and the current between drain and source is monitored with a chart recorder. Typical current waveforms [3] for a commercial five-minute epoxy curing at room temperature are shown in Figure 2. In the sequence shown, the gate voltage is applied for 30 seconds, then turned off for 30 seconds. Thus one waveform is obtained each minute during the cure cycle. Until 4 minutes have passed, the waveform resembles what is illustrated in Fig. 2 for the 4 minute result. A sharp peak is observed when the gate voltage is applied that decays rapidly to a much lower final value. At about 7 minutes, the nominal cure time, this decay begins slowing down, and the peak value reduces in amplitude. By 10 minutes, a finite delay time between the application of the gate voltage and the appearance of current is clearly visible, and the peak shows a slow rise and even slower fall. By 13 minutes, the peak has disappeared, and the shape of the curve has stabilized in the form shown, with a long delay and a gradual rise to a final current.

When first obtained, waveforms such as those in Fig. 2 were difficult

FIGURE 2

4.

I_{ds}

V_g

4 min   5min   6min   7 min   8 min

I_{ds}

V_g

9min   10min   11min   12min   13min
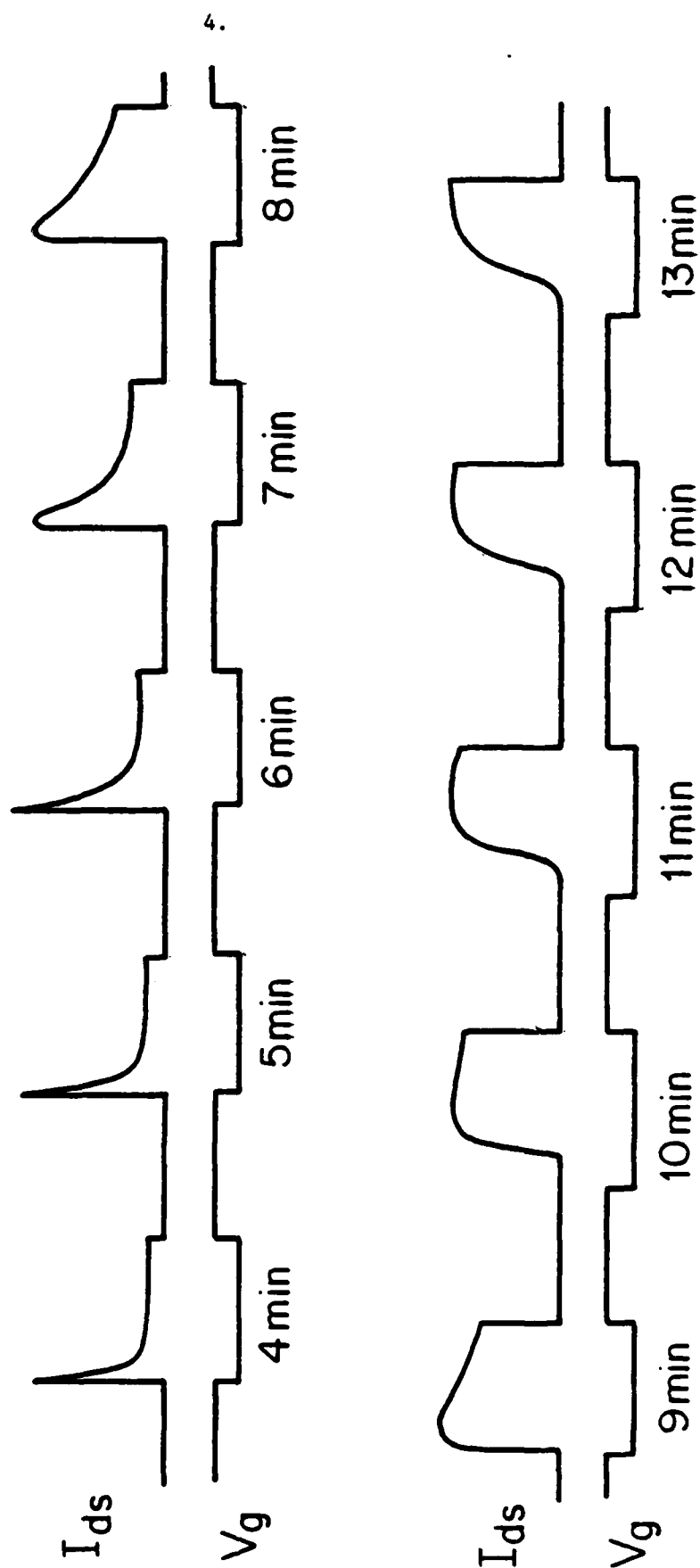
to understand. Previous experience [1] in using extremely thin polymer films (0.1 micron) as gate materials gave no indication of the large peaks encountered with the resins. The program of experiments reported here was directed toward a more complete documentation of the waveform features and the development of a model that can account for what is observed. A relatively well-characterized commercial resin was studied at various cure temperatures, and corresponding measurements of the dielectric constant and loss tangent were made. The origin of the peak in the current waveforms during the early part of the cure cycle was successfully identified, and resulted in the development of a physically reasonable circuit model with which the observed behavior can be explained.

II. EXPERIMENTAL PROCEDURES

The epoxy resin used in the present set of experiments is the same commercial formulation referred to as Resin I in recent studies by Schneider et al. [4] and by Senich et al. [5]. The epoxy components are cresol novolac, diglycidyl ether of bisphenol-A, and t-butylphenyl glycidyl ether. The amine curing agent is dicyandiamide. A urea-type accelerator is also present. The mixture is a tacky solid at room temperature. Recommended cure is two hours at 127 °C. This resin was selected partly because of the availability of cure-characterization data, and partly because it was convenient to use: it can be premixed and stored, and it cures at convenient temperatures.
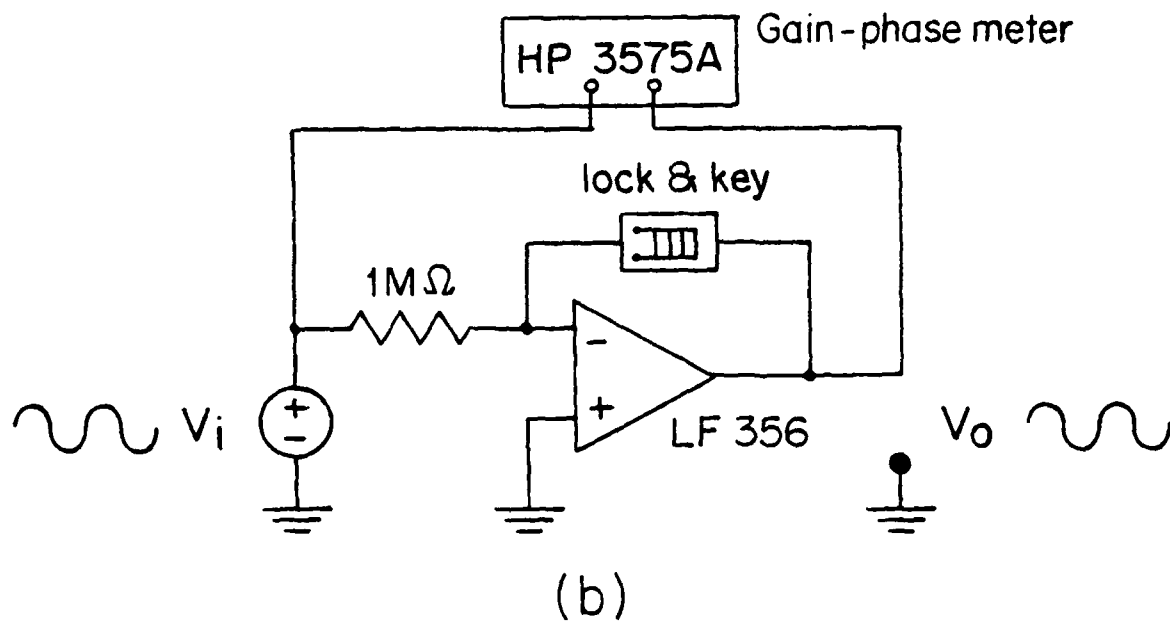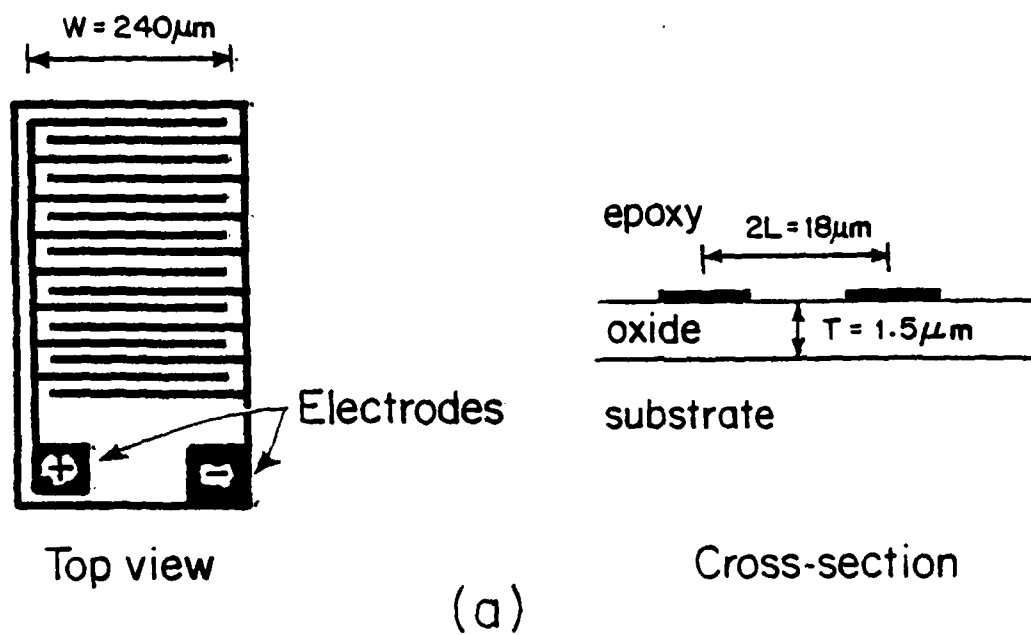
Two types of studies were made on this resin: CFT waveforms were monitored during cure at several different temperatures for devices with several different gate-gap widths, and low frequency dielectric constant and loss tangent were measured during cure using a planar interdigitated electrode structure (Fig 3a). Each electrode contains eighteen fingers, 240 μm by 9 μm, and the interelectrode gap is 9 μm.

Both types of test devices were fabricated on 75 mil square silicon chips [6]. Each chip was bonded to a standard TO-99 transistor header. The mounted device was placed in an oven which was then brought to temperature. An experiment was begun by contacting the solid resin to the hot chip so that the resin flowed over the entire surface. The sample size obtained in this way was on the order of a milligram. The oven temperature was monitored with a thermocouple adjacent to the device, and was maintained to within ± 1 °C of the desired value. Dry nitrogen was passed through the oven during the experiment.

The CFT waveforms were monitored during cure cycles at 100°, 110°, and 120° for gate-gap widths of 0.25, 0.5, 0.75, 1.25 and 1.5 mils. A voltage of amplitude -25 V was applied to the gate every three minutes for an interval of 30 seconds. Current waveforms were recorded for each gate voltage application.

Experiments to measure ε', ε'', and tan δ with the interdigitated electrode structure were done over the range 80-120 °C at 1000 Hz. The device, also referred to as a lock-and-key structure, was connected as the feedback element in the inverting amplifier (Fig. 3b), so that
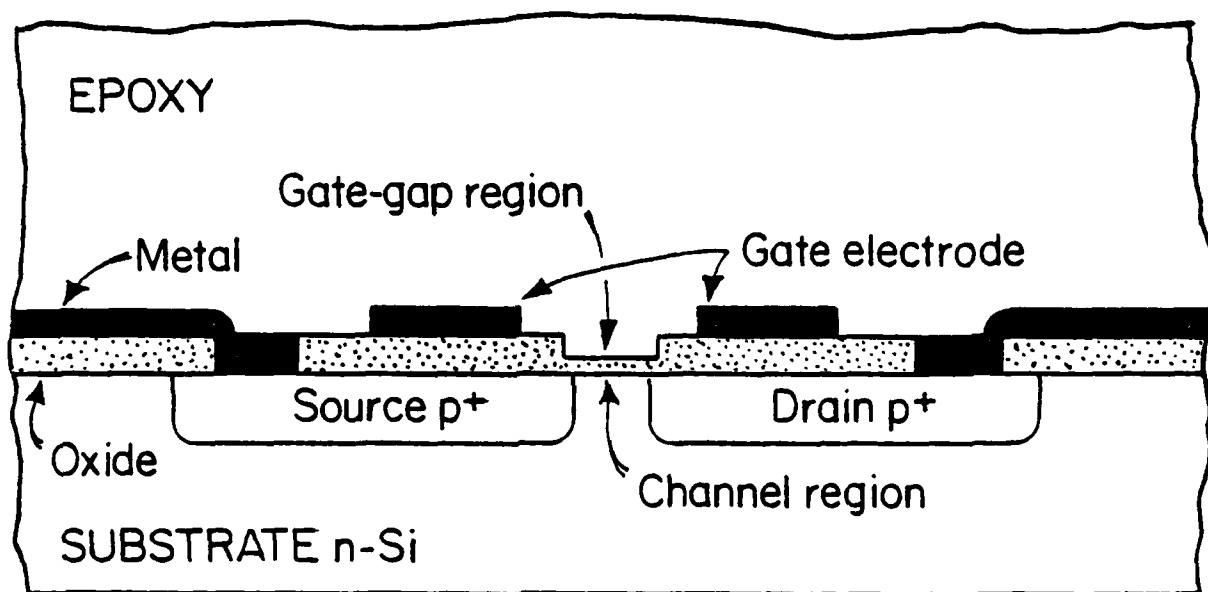
FIGURE 3

W = 240μm

epoxy   2L = 18μm

oxide   T = 1.5μm

substrate

Electrodes

Top view

Cross-section

(a)

HP 3575A   Gain-phase meter

lock & key

1MΩ

Vi

LF 356   Vo

(b)

measurements were made at constant current, rather than at the more normally used constant voltage. An HP 3575A gain-phase meter was used to monitor the device admittance during cure. It should be pointed out that because of the large loss tangents in the early phases of cure, conventional capacitance meters cannot be used for this measurement. The gain-phase meter works extremely well when both the real and imaginary parts of the dielectric constant are appreciable, but it is less precise than a capacitance bridge in the determination of small ϵ'' and hence small loss tangents. This means we are able to follow the cure to and beyond gelation quite well, but lose sensitivity in the final curing stages.

After the first complete set of measurements were made, a model was formulated that ascribed the peaks in the CFT waveforms to direct capacitive coupling between the gate electrode and the CFT channel. To test this hypothesis, an additional CFT test was also performed using a modified CFT structure due to Togashi and Senturia [7]. A cross-section of this device is shown in Fig. 4. Note that the gate electrode is set well over the source and drain regions, so that there is no overlap between the metal electrodes and the channel region. The operating principle of this device is identical to the original CFT structure, except for the absence of direct capacitive coupling between electrode and channel. Because the metal does not overlap the channel it is possible to observe both turn-on and turn-off waveforms with this device. It will be shown below that, indeed, there are no peaks in the CFT waveforms obtained for this structure, thus verifying our identification of

FIGURE 4

EPOXY

Gate-gap region

Metal

Gate electrode

Oxide

Source p+

Drain p+

Channel region

SUBSTRATE n-Si

the peaks' origin.

III   EXPERIMENTAL RESULTS

A.   Charge-flow transistors

Figures 5 and 6 show typical sequences of drain-current response to the gate voltage signal for gate-gap widths of 0.25, 0.75 and 1.25 mils at one temperature. A total of twenty-five such tests, covering five gap widths and three temperatures, were made. Initially, the shape of the current response is the same for all devices, with magnitude inversely proportional to gap width. During subsequent cycles, the current waveform is the same shape, but the magnitude of the current decreases. The 1.25 mil devices eventually turn off and remain off. The 0.25 and 0.75 mil devices show more complex behavior, the magnitude of the current eventually increasing with subsequent cycles until the waveforms resemble those obtained with thin polymer films. The final response of the 0.25 mil device is nearly identical to the response of the same device to dry nitrogen, measured before the epoxy was applied. The response of the 0.75 mil device during the later stages of cure shows an increasing turn-on delay with subsequent cycles until the device remains off during the 30 second gate voltage pulse.

The sequences described above are thermally activated, in that the general time scale for the observed sequences roughly halves for each
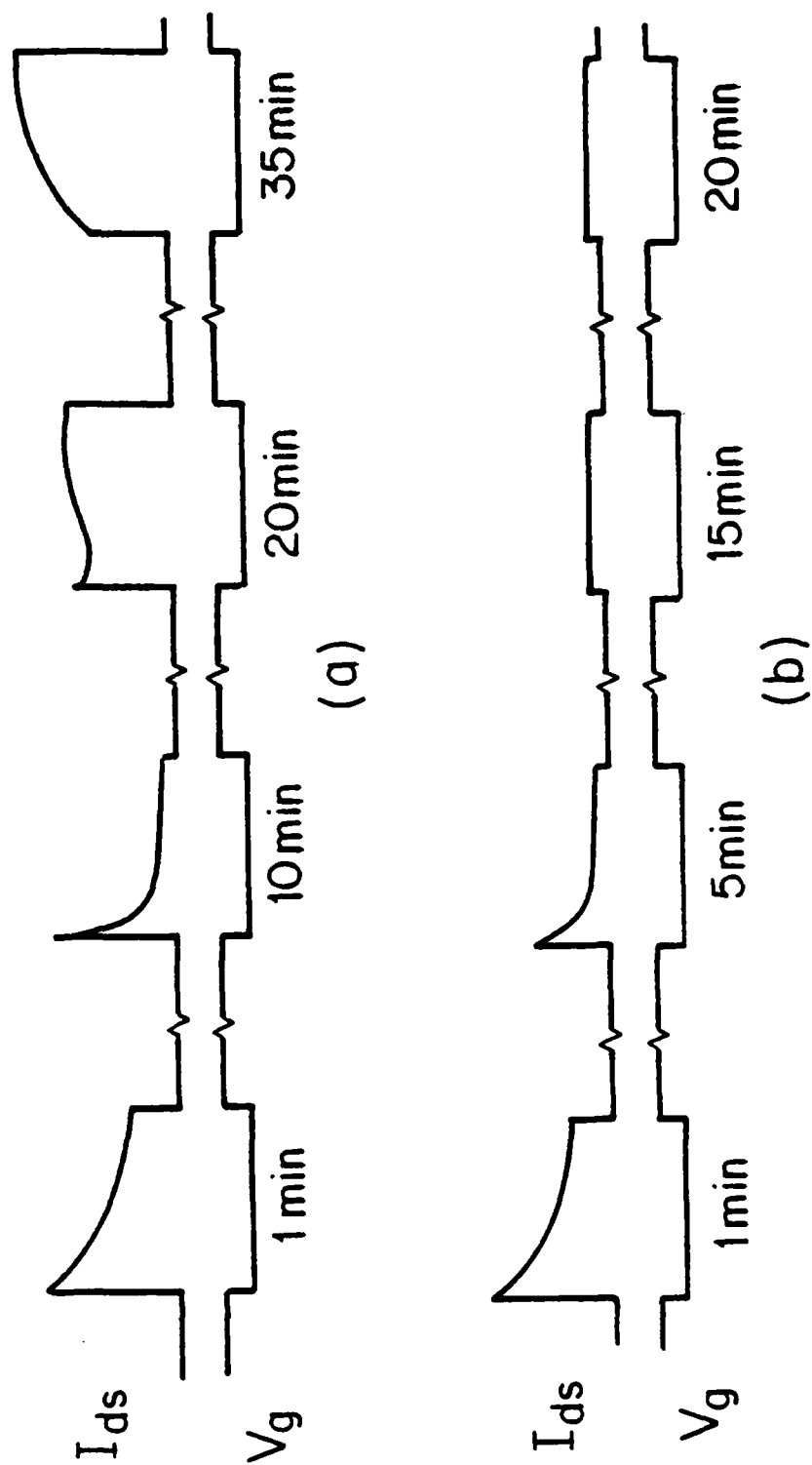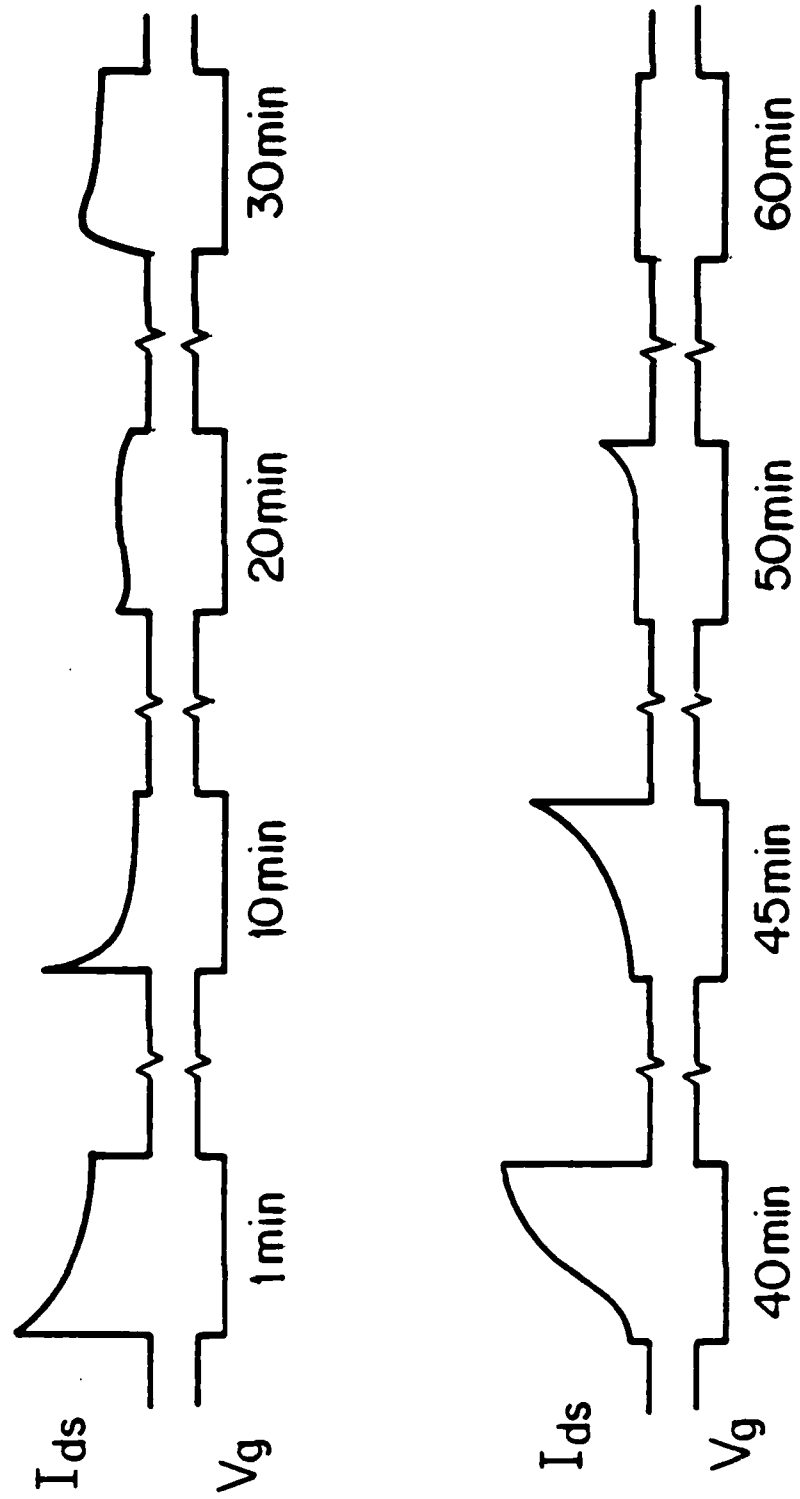
FIGURE 5

(a)

(b)

FIGURE 6

10 °C increase in cure temperature, which would correspond to an activation energy on the order of 20 kcal/gmole, but in these preliminary measurements, it has not yet been possible to identify a specific event in the waveform with which to make a more precise determination of activation energy.

Corresponding waveforms for the modified CFT structure of Fig. 4 are shown in Fig. 7. It is seen that the prominent peak in the data of Figs. 5 and 6 is absent here, which as will be discussed in detail below, serves to identify the origin of the peak. Otherwise, the general trend in the data is what one would expect -- a gradual slowing down of the turn-on and turn-off phenomena during cure.

B. Interdigitated Electrode

Senturia [8] has derived an expression for the admittance of a lock and key device covered with a thin polymer film. The result can be modified to account for the resin, the thickness of which is assumed infinite, yielding an admittance,

$$Y = G + j\omega C$$

where

$$G = \frac{4\sqrt{2}NW}{\pi^2} \left[\sigma_{resin} + \sigma_{sub} + \frac{\pi T}{L}\sigma_{ox} + \frac{\pi}{L}(\kappa_{ox} + \varsigma_{sub})\right]$$

$$C = \frac{4\sqrt{2}NW}{\pi^2} \left[\varepsilon_{resin} + \varepsilon_{sub} + \frac{\pi T}{L}\varsigma_{ox}\right]$$

FIGURE 7

I_{ds}

V_g

1min   5min   9min

I_{ds}

V_g

13min   17min   21min
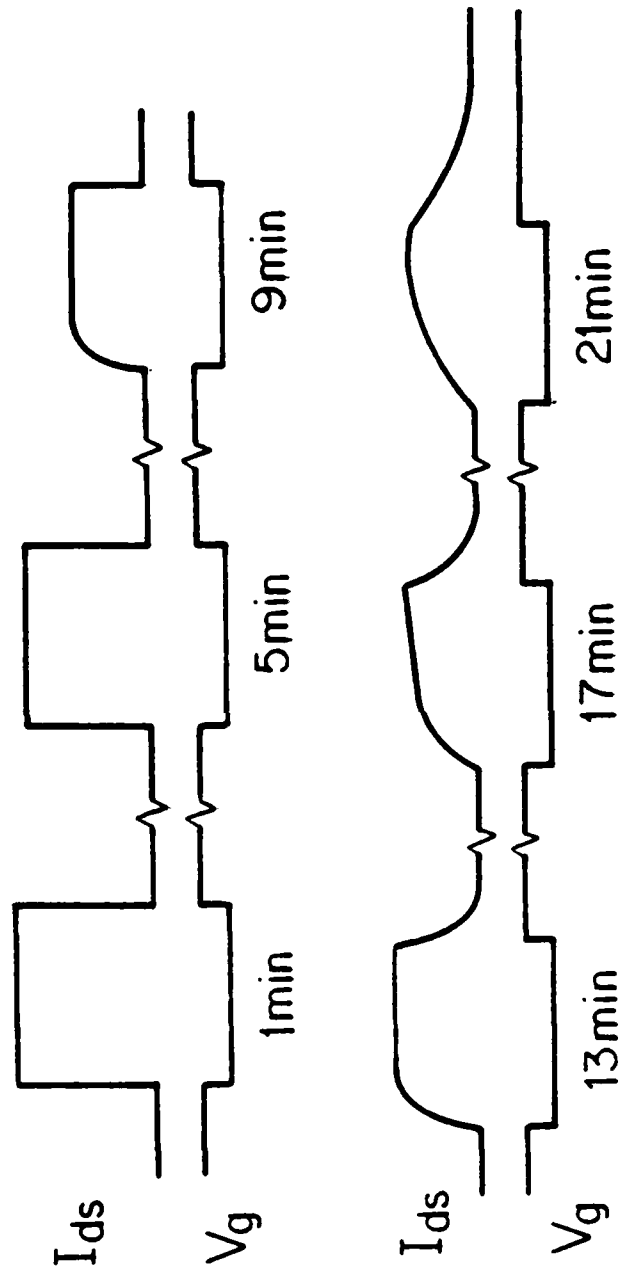
and

N = total number of interelectrode gaps

W = length of electrodes

L = interelectrode separation

T = oxide layer thickness

σ = conductivity

ε = dielectric permittivity

κ_{ox} = surface conductivity at oxide-resin interface

κ_{sub} = surface conductivity at substrate-oxide interface

The above expressions were set equal to the conductance G and capacitance C determined experimentally, and solved for $\varepsilon' = \varepsilon_{resin}$, $\varepsilon'' = \sigma_{resin}/\omega$ and $\tan\delta = \varepsilon''/\varepsilon'$. The constants in the expressions are fit to the data by measuring the admittance of the uncoated lock and key and substituting $\varepsilon_{resin} = \varepsilon_o$ (8.85 x 10^{-12} F/m) and $\sigma_{resin} = 0$. The accuracy of ε', ε'' and $\tan\delta$ determined in this way is expected to decrease with decreasing ε_{resin} and σ_{resin}, and will be least accurate in the final stages of cure.

The dependence of ε' and ε'' on cure time and temperature is illustrated in Fig. 3. The initial rise may be due to increasing concentration of hydroxyl groups as a reaction product. A rapid increase in viscosity due to the onset of gelation causes the sharp decrease in the curves. The progressive shift towards longer time for decreasing cure temperature is due to the thermal activation of the curing reaction. The breaks in the curves seem to correlate with the time to gelation t_g

FIGURE 8
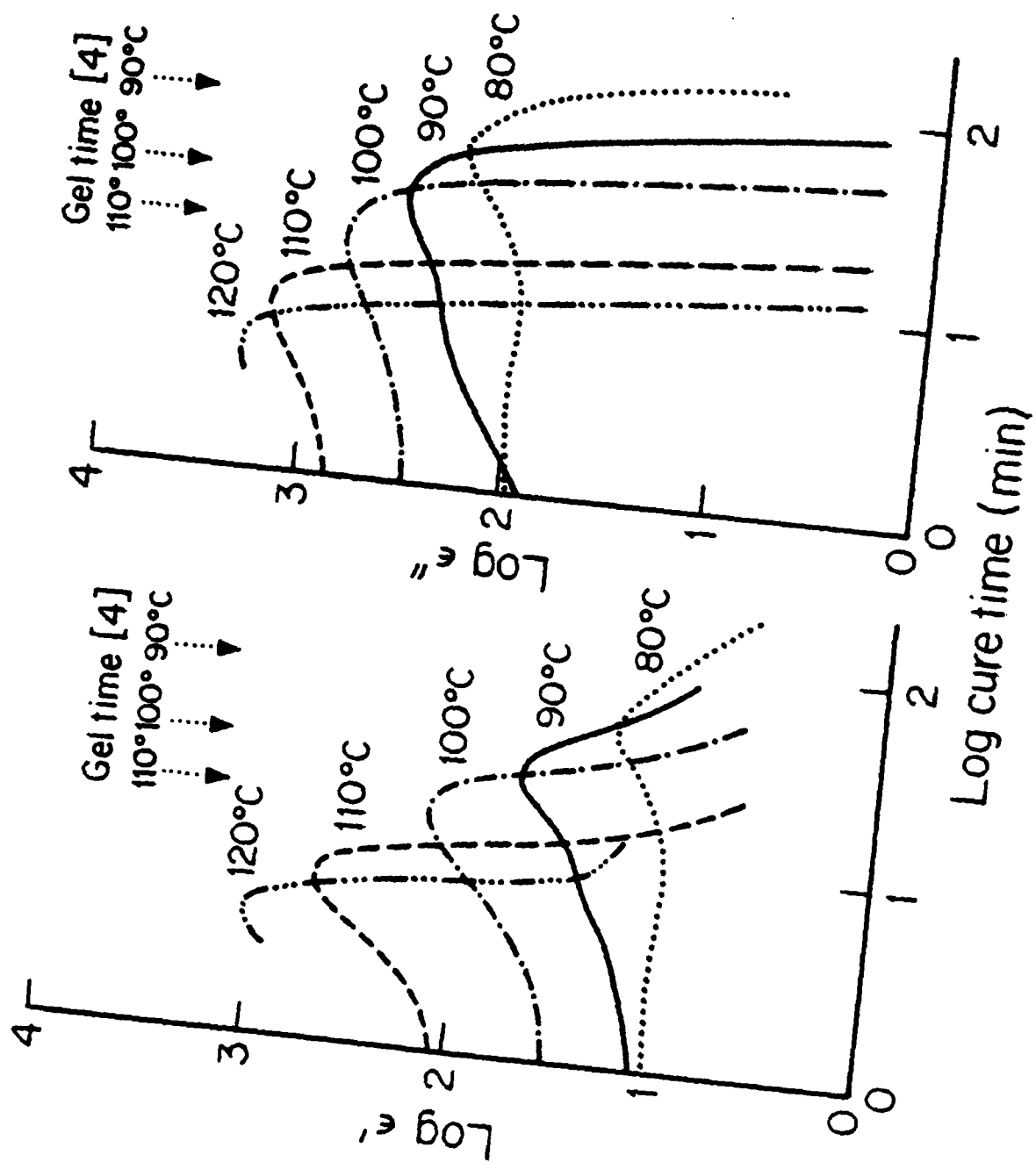
determined by Schneider et al. [4], using torsional braid analysis, as indicated on Fig. 8. The higher viscosity that results from lower cure temperature would explain the decreasing magnitude of ε' and ε'' with decreasing cure temperature.

The behavior of tan δ with cure temperature is shown in figure 9. The dissipation factor falls initially to a minimum, rises again to a peak and then falls off sharply. Delmonte [9] attributed the loss maximum to the gelation of the resin. However, electrical [10] and mechanical [5] studies suggest the peak is due to the attainment of a critical vicosity, which is frequency dependent. The elasped times to the loss maxima in Fig. 9, t_{max}, can be used to determine an activation energy for the curing process [5]. The slope of a plot of $\ln(t_{max})$ vs $1/T$ (Fig. 10) yields a value of 17.8 kcal/mole, which agrees favorably with the values of 20.3, 19.7, and 21.0 kcal/mole determined by DSC, TBA and DSA respectively [4], [5].

IV. DISCUSSION AND CONCLUSION

A. The Model

A simple circuit model of the resin coated charge-flow transistor can account for the variation of the drain current response with cure. The model is illustrated in Figure 11. The physical interpretation of each element is:

FIGURE 9

FIGURE 9

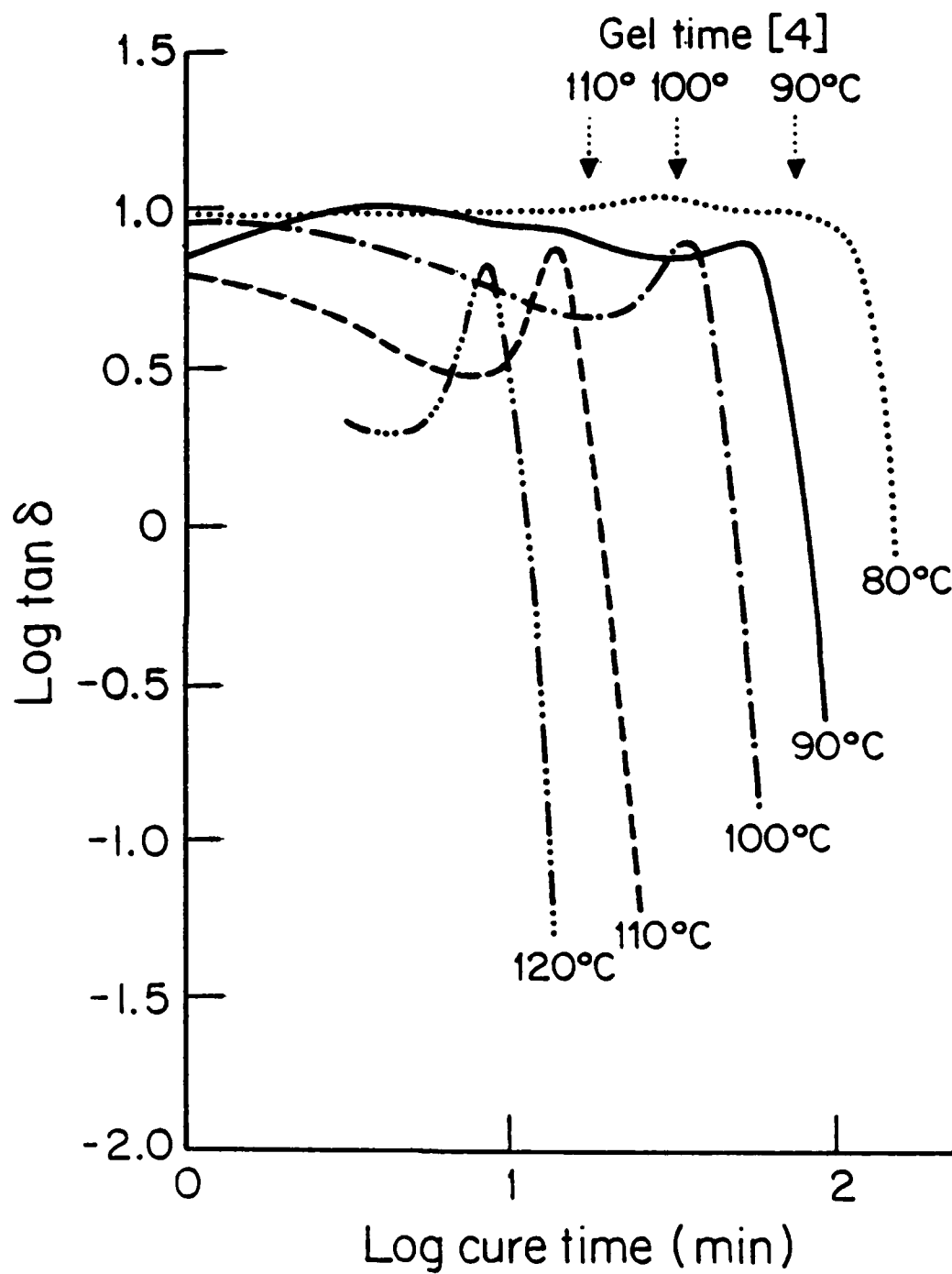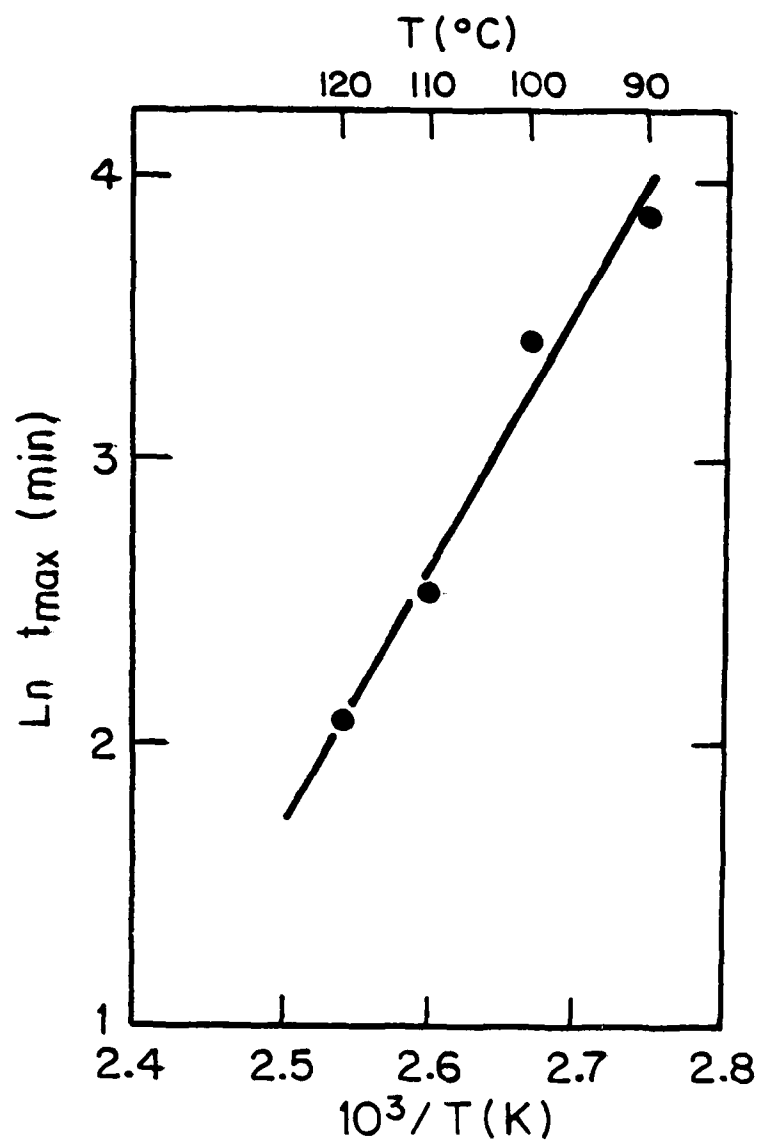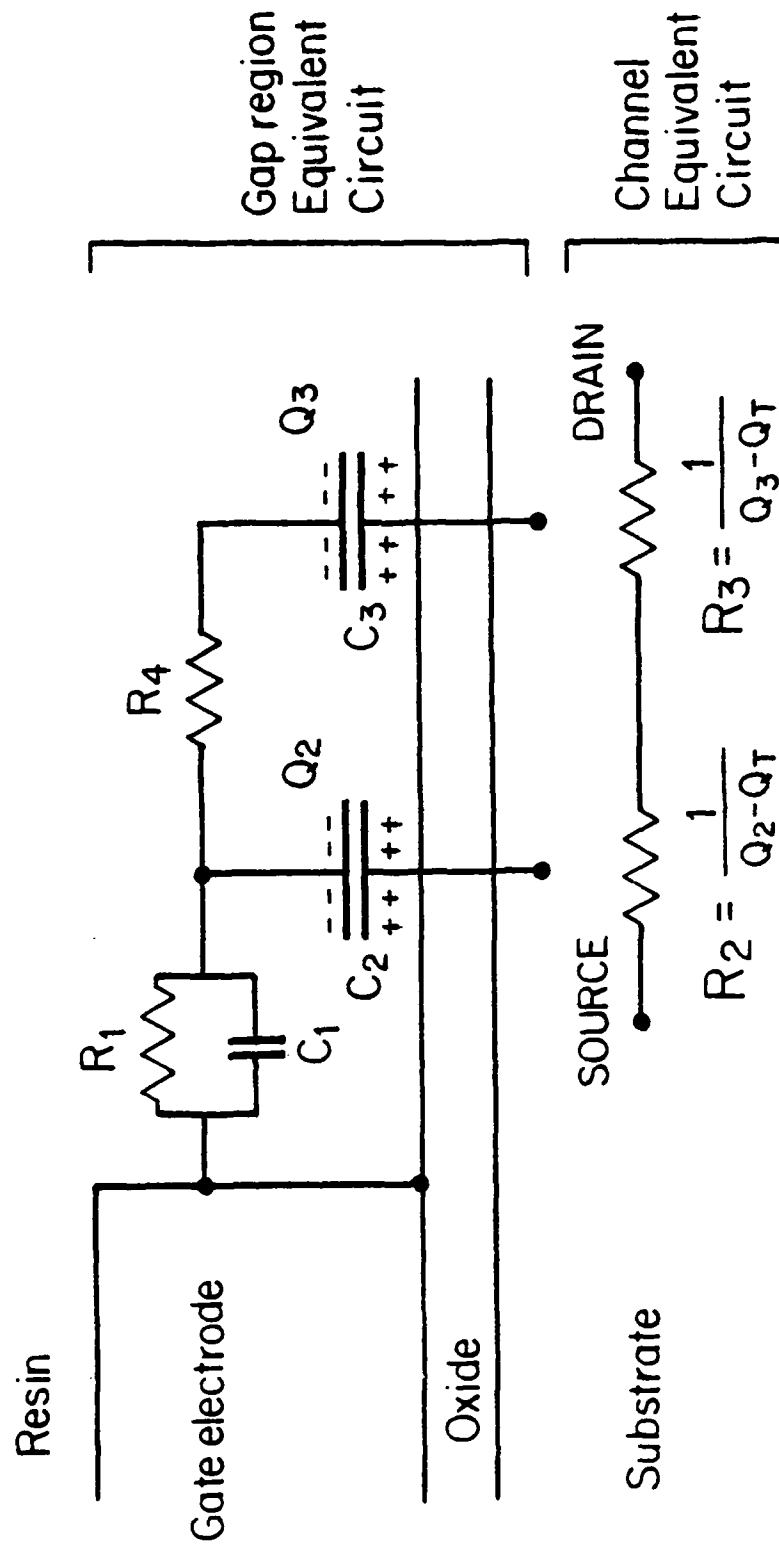FIGURE 10

20.

FIGURE 11

Resin

Gate electrode

Oxide

Substrate

R_1

C_1

C_2

Q_2

R_4

C_3

Q_3

Gap region
Equivalent
Circuit

Channel
Equivalent
Circuit

SOURCE

DRAIN

$R_2 = \dfrac{1}{Q_2 - Q_T}$

$R_3 = \dfrac{1}{Q_3 - Q_T}$

C_1 - The contact capacitance of the ionic dipole layer (or, later in the cure, perhaps electronic dipole layer) at the epoxy-electrode interface. The value of C_1 is expected to decrease during cure due to decreasing ion concentration and mobility.

R_1 - The contact resistance represents the ability of the electrode to inject charge into the resin. This may depend on resin properties, and it may be determined by oxide formation on the electrode.

C_2 - An electrode-to-near-channel capacitance that is due to direct capacitive coupling between the gate electrode and the channel region beneath the resin. It may be dependent on the resin properties.

R_4 - The bulk resin resistance, which represents the resistance through which the mid-channel region is coupled to the gate electrode. This resistance depends strongly on the resin resistivity.

C_3 - A resin-to-mid-channel capacitance that is coupled to the electrode through R_4. This capacitance depends strongly on the resin dielectric constant.

R_2, R_3 - Lumped elements representing the channel resistance, and thus which determine the drain current flowing through the device. The value of the resistance is inversely proportional to the mobile charge in the portion of the channel represented by

each resistor. This mobile charge is equal to the total
charge Q less a threshold charge Q_T needed just to form a
channel.

The total resistance of the channel is $R_2 + R_3$, and the drain current will
be proportional to the channel conductance. Thus the drain current has
the form

$$I_D \; \alpha \; \frac{1}{R_2 + R_3} \; = \; \frac{1}{\dfrac{1}{Q_2 - Q_T} + \dfrac{1}{Q_3 - Q_T}}$$

for $Q_2 > Q_T$ and $Q_3 > Q_T$, $I_D = 0$ otherwise.

The response of the network in Fig. 11 to an applied step of
voltage can be calculated using ordinary linear network theory, and the
quantity

$$I = \frac{1}{1/Q_2 + 1/Q_3}$$

computed as a function of time for various choices of model parameters.

B. Discussion of Results

The model described above was selected as the simplest assembly of
lumped elements that could reasonably represent the distributed RC trans-
mission line of the resin-to-channel structure, the coupling between
electrode and resin, and the coupling between electrode and channel. The

significant, and perhaps non-obvious part of this model, is the fact that the channel conductance is a nonlinear function of the charges on the two capacitors C_2 and C_3, and because of this nonlinearity, it is possible to obtain peaked waveforms even when the linear electrode-to-channel circuit is driven with a simple step function. The recognition of this detail permitted the successful development of what, in hindsight, is a straightforward and physically reasonable model.

In order to illustrate the properties of this model, we consider first the data on the resin's dielectric properties obtained from the interdigitated electrode measurements. We see that both ϵ' and ϵ'' are large during the early part of the cure cycle, and both drop sharply after gelation. Using these facts, and using the identification of C_3 and R_4 as the elements that should depend most strongly on the resin's properties, it is reasonable to try as a first-order guess that C_3 should behave like ϵ' and R_4 should behave like $1/\epsilon''$ (ϵ'' is proportional to conductivity). Since both ϵ' and ϵ'' behave similarly during curing, we can estimate that the $R_4 C_3$ product should be roughly constant during cure, but C_3 should drop sharply and R_4 should rise sharply.

We have used this reasoning to calculate a sequence of model waveforms for fixed C_1, R_1, and C_2, but with varying C_3 and R_4 such that the $R_4 C_3$ product is constant. For these calculations, we have assumed $Q_T = 0$. The model waveforms are shown in Fig. 12. Note how the peak in the "early" portions of cure (C_3 large, R_4 small) goes over into the gradual turn-on the "late" portions of cure (C_3 small, R_4 large).

FIGURE 12
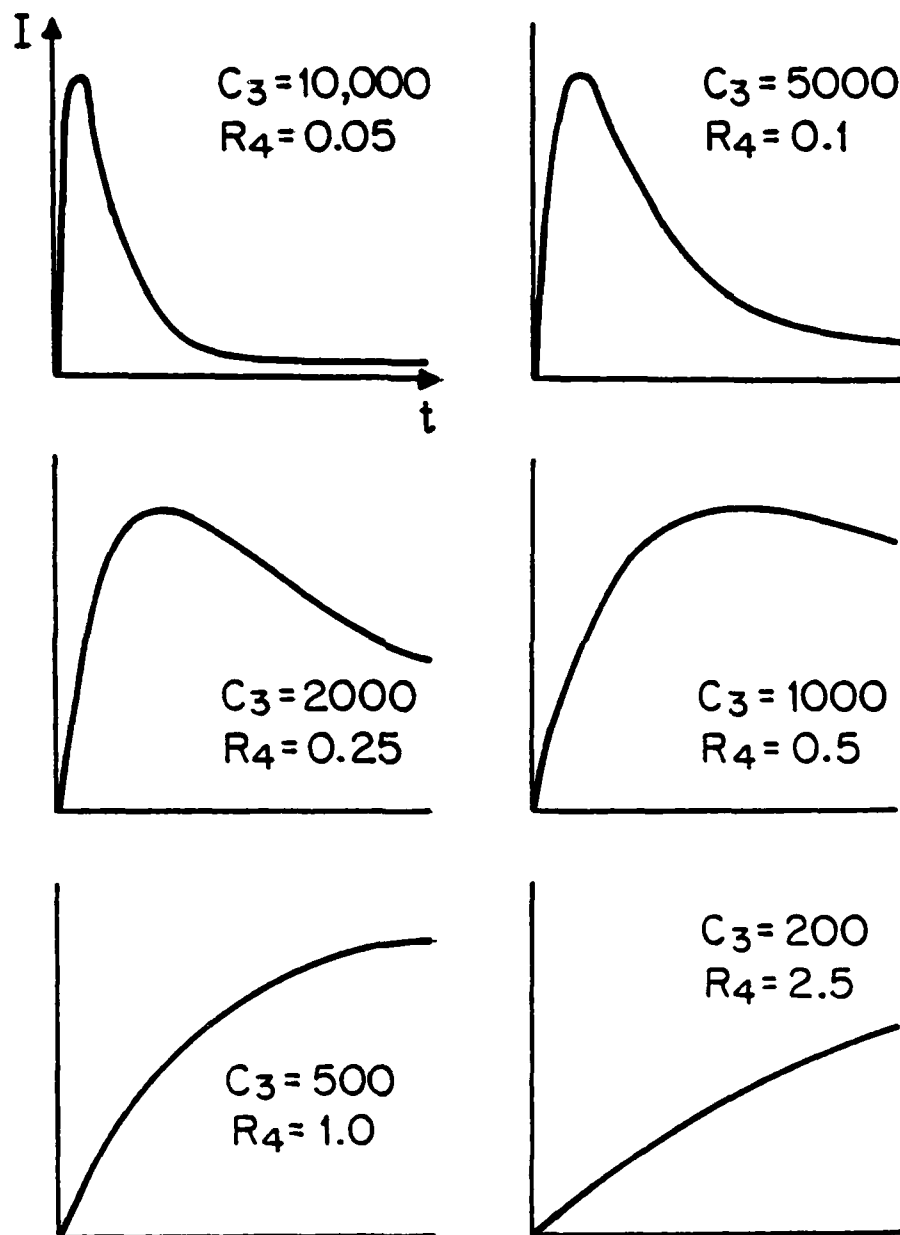
The similarity between the model waveforms of Fig. 12 and the data of Figs. 2, 5 and 6 is obvious. In physical terms, the origin of the peak is as follows: When the gate voltage is turned on, the capacitive voltage divider between C_1 and C_2 couples some charge into C_2 very quickly. This charge redistributes between C_2 and C_3 at a rate determined by the resistance R_4. As a result, the portion of the channel beneath C_2, initially turned strongly on by the gate pulse, becomes more resistive as the portion of the channel beneath C_2 becomes less resistive. That is, on a time scale short compared to the time required for charge injection into the resin through R_1, the charging of C_3 must be accompanied by a partial discharging of C_2. Since the channel conductance is a function of both states of charge, the peaking occurs when the two charge-controlled channel resistors R_2 and R_3 are similar in magnitude.

As a confirmation of the identification of the origin of the peak, the modified CFT of Fig. 4 is built such that C_2 does not affect the channel conductance, only C_3. The fact that the peak is absent from these waveforms (Fig. 7) confirms the origin of the peak.

We believe that this model correctly accounts for the most prominent features of the observed waveforms, and when coupled with dielectric data, shows that these features are directly related to basic physical changes in the resin during cure. The next phase of this effort will be devoted to making a quantitative link between the detailed waveforms and the dielectric properties of the resins.

ACKNOWLEDGEMENT

REFERENCES

1. S.D. Senturia, C.M. Sechen and J.A. Wishneusky, Appl. Phys. Lett.,
   30, 106, (1977).

2. The suggestion that such monitoring might be possible originated
   with Dr. L.H. Peebles, Jr., of the Office of Naval Research.

3. H. Appelman, M.I.T. Internal Memorandum, unpublished.

4. N.S. Schneider, J.F. Sprouse, G.L. Hagnauer and J.K. Gillham,
   Polym. Eng. Sci., 19, 304 (1979).

5. G.A. Senich, W.J. MacKnight and N.S. Schneider, Polym. Eng. Sci.,
   19, 313 (1979).

6. The CFT devices were fabricated by L. Bowen and N. Sheppard in the
   Microelectronics Laboratory Central Facility of the M.I.T. Center
   for Materials Science and Engineering. The interdigitated elec-
   trode structures were fabricated at Hewlett-Packard Deer Creek
   Laboratories as part of a multi-element chip designed in the Fall
   of 1978 by L. Bowen, J. Rubinstein, S. Azoury and S. Senturia for
   an M.I.T. Course in L.S.I. design, taught by L. Conway of Xerox
   Palo Alto Research Center, which also sponsored the course.

7. Kou Togashi, S.B. Thesis, M.I.T., 1979, unpublished.

8. S.D. Senturia, NASA CR-134764, Final Contract Report, April 1975.

9. J. Delmonte, J. Appl. Polym. Sci., 2, 108 (1965).

10. E.N. Haran, H. Gringas and D. Katz, J. Appl. Polym. Sci., 9, 3505
    (1965).

TECHNICAL REPORT DISTRIBUTION LIST, GEN

	No. Copies		No. Copies
Office of Naval Research Attn: Code 472 800 North Quincy Street Arlington, Virginia 22217	2	U.S. Army Research Office Attn: CRD-AA-IP P.O. Box 1211 Research Triangle Park, N.C. 27709	1
ONR Branch Office Attn: Dr. George Sandoz 536 S. Clark Street Chicago, Illinois 60605	1	Naval Ocean Systems Center Attn: Mr. Joe McCartney San Diego, California 92152	1
ONR Branch Office Attn: Scientific Dept. 715 Broadway New York, New York 10003	1	Naval Weapons Center Attn: Dr. A. B. Amster, Chemistry Division China Lake, California 93555	1
ONR Branch Office 1030 East Green Street Pasadena, California 91106	1	Naval Civil Engineering Laboratory Attn: Dr. R. W. Drisko Port Hueneme, California 93401	
ONR Branch Office Attn: Dr. L. H. Peebles Building 114, Section D 666 Summer Street Boston, Massachusetts 02210	1	Department of Physics & Chemistry Naval Postgraduate School Monterey, California 93940	
Director, Naval Research Laboratory Attn: Code 6100 Washington, D.C. 20390	1	Dr. A. L. Slafkosky Scientific Advisor Commandant of the Marine Corps (Code RD-1) Washington, D.C. 20380	1
The Assistant Secretary of the Navy (R,E&S) Department of the Navy Room 4E736, Pentagon Washington, D.C. 20350	1	Office of Naval Research Attn: Dr. Richard S. Miller 800 N. Quincy Street Arlington, Virginia 22217	1
Commander, Naval Air Systems Command Attn: Code 310C (H. Rosenwasser) Department of the Navy Washington, D.C. 20360	1	Naval Ship Research and Development Center Attn: Dr. G. Bosmajian, Applied Chemistry Division Annapolis, Maryland 21401	1
Defense Documentation Center Building 5, Cameron Station Alexandria, Virginia 22314	12	Naval Ocean Systems Center Attn: Dr. S. Yamamoto, Marine Sciences Division San Diego, California 91232	1
Dr. Fred Saalfeld Chemistry Division Naval Research Laboratory Washington, D.C. 20375	1	Mr. John Boyle Materials Branch Naval Ship Engineering Center Philadelphia, Pennsylvania 19112	1

TECHNICAL REPORT DISTRIBUTION LIST. GEN

No.
Copies

Dr. Rudolph J. Marcus
Office of Naval Research
Scientific Liaison Group
American Embassy
APO San Francisco   96503   1

Mr. James Kelley
DTNSRDC Code 2803
Annapolis, Maryland   21402   1

TECHNICAL REPORT DISTRIBUTION LIST, 356A

	No. Copies		No. Copies
Dr. Stephen H. Carr Department of Materials Science Northwestern University Evanston, Illinois 60201	1	Picatinny Arsenal SMUPA-FR-M-D Dover, New Jersey 07801 Attn: A. M. Anzalone Building 3401	1
Dr. M. Broadhurst Bulk Properties Section National Bureau of Standards U.S. Department of Commerce Washington, D.C. 20234	2	Dr. J. K. Gillham Princeton University Department of Chemistry Princeton, New Jersey 08540	1
Dr. T. A. Litovitz Department of Physics Catholic University of America Washington, D.C. 20017	1	Douglas Aircraft Co. 3855 Lakewood Boulevard Long Beach, California 90846 Attn: Technical Library C1 290/36-84 AUTO-Sutton	
Professor G. Whitesides Department of Chemistry Massachusetts Institute of Technology Cambridge, Massachusetts 02139	1	Dr. E. Baer Department of Macromolecular Science Case Western Reserve University Cleveland, Ohio 44106	1
Professor J. Wang Department of Chemistry University of Utah Salt Lake City, Utah 84112	1	Dr. K. D. Pae Department of Mechanics and Materials Science Rutgers University New Brunswick, New Jersey 08903	1
Dr. V. Stannett Department of Chemical Engineering North Carolina State University Raleigh, North Carolina 27607	1	NASA-Lewis Research Center 21000 Brookpark Road Cleveland, Ohio 44135 Attn: Dr. T. T. Serofini, MS-49-1	1
Dr. D. R. Uhlmann Department of Metallurgy and Material Science Massachusetts Institute of Technology Cambridge, Massachusetts 02139	1	Dr. Charles H. Sherman, Code TD 121 Naval Underwater Systems Center New London, Connecticut	
Naval Surface Weapons Center White Oak Silver Spring, Maryland 20910 Attn: Dr. J. M. Augl Dr. B. Hartman	1	Dr. William Risen Department of Chemistry Brown University Providence, Rhode Island 02192	
Dr. G. Goodman Globe Union Incorporated 3757 North Green Bay Avenue Milwaukee, Wisconsin 53201	1	Dr. Alan Gent Department of Physics University of Akron Akron, Ohio 44304	

TECHNICAL REPORT DISTRIBUTION LIST, 356A

	No. Copies		No. Copies

Mr. Robert W. Jones
Advanced Projects Manager
Hughes Aircraft Company
Mail Station D 132
Culver City, California 90230   1

Dr. C. Giori
IIT Research Institute
10 West 35 Street
Chicago, Illinois 60616   1

Dr. M. Litt
Department of Macromolecular Science
Case Western Reserve University
Cleveland, Ohio 44106   1

Dr. R. S. Roe
Department of of Materials Science
  and Metallurgical Engineering
University of Cincinnati
Cincinnati, Ohio 45221   1

Dr. Robert E. Cohen
Chemical Engineering Department
Massachusetts Institute of Technology
Cambridge, Massachusetts 02139   1

Dr. David Roylance
Department of Materials Science and
  Engineering
Massachusetts Institute of Technology
Cambridge, Massachusetts 02039   1

Dr. T. P. Conlon, Jr., Code 3622
Sandia Laboratories
Sandia Corporation
Albuquerque, New Mexico   1

Dr. Martin Kaufmann, Head
Materials Research Branch, Code 4542
Naval Weapons Center
China Lake, California 93555   1

Dr. T. J. Reinhart, Jr., Chief   1
Composite and Fibrous Materials Branch
Nonmetallic Materials Division
Department of the Air Force
Air Force Materials Laboratory (AFSC)
Wright-Patterson Air Force Base, Ohio 45433

Dr. J. Lando
Department of Macromolecular Science
Case Western Reserve University
Cleveland, Ohio 44106

Dr. J. White
Chemical and Metallurgical Engineering
University of Tennessee
Knoxville, Tennessee 37916

Dr. J. A. Manson
Materials Research Center
Lehigh University
Bethlehem, Pennsylvania 18015   1

Dr. R. F. Helmreich
Contract RD&E
Dow Chemical Co.
Midland, Michigan 48640   1

Dr. R. S. Porter
University of Massachusetts
Department of Polymer Science and
  Engineering
Amherst, Massachusetts 01002   1

Professor Garth Wilkes
Department of Chemical Engineering
Virginia Polytechnic Institute and
  State University
Blacksburg, Virginia 24061   1

Dr. Kurt Baum
Fluorochem Inc.
6233 North Irwindale Avenue
Azuza, California 91702

Professor C. S. Paik Sung
Department of Materials Sciences and
  Engineering Room 8-109
Massachusetts Institute of Technology
Cambridge, Massachusetts 02139

2